Journal of Engineering Mathematics, Vol. 13, No. 2, April 1979

© 1979 Sijthoff & Noordhoff International Publishers – Alphen aan den Rijn
Printed in the Netherlands

Computation of electromagnetic fields scattered by a cylindrical inhomogeneity in a homogeneous medium of infinite extent

G. MUR

Department of Electrical Engineering, Delft University of Technology, Delft, The Netherlands.

(Received June 12, 1978)

SUMMARY

A method is presented for computing time harmonic electromagnetic fields scattered by a cilindrical inhomogeneity in a homogeneous medium of infinite extent. Geometrically, the homogeneity is a cylinder of arbitrary cross-section. Outside a circular cylinder that completely surrounds the inhomogeneity, the electromagnetic field is expanded in terms of wave functions of the circular cylinder. Inside this cylinder, the electromagnetic field equations are transformed into a system of ordinary differential equations in the 'radial' direction. The relevant system behaves numerically unstable and is therefore transformed into a stable one through a specific transformation scheme. To elucidate the validity and the versatility of the method, numerical results are presented for fields scattered by a number of different cylindrical inhomogeneities.

1. Introduction

In this paper, a method is presented for computing time-harmonic electromagnetic fields scattered by a cylindrical inhomogeneity in a homogeneous medium of infinite extent. The dielectric and/or magnetic properties of the inhomogeneity are assumed to be independent of the longitudinal Cartesian coordinate z (see Fig. 1), but may vary with the transverse polar coordinates r and ϕ. Geometrically, the inhomogeneity is a cylindrical object of arbitrary cross-section. The incident electromagnetic field is due to sources located outside a circular cylinder of radius r_1 and the z-axis as axis, that completely surrounds the inhomogeneity. Outside this circular cylinder (i.e. in Region I), the electromagnetic fields are expanded in terms of the wave functions of the circular cylinder. Inside the cylinder, the electromagnetic-field equations are transformed into a system of first-order ordinary differential equations in the radial variable r. The medium in a cylinder of radius r_2 and the z-axis, where $0 < r_2 \leqslant r_1$, is assumed to be homogeneous again and consequently, the field inside this cylinder, too, can be expressed in terms of cylindrical wave functions, which facilitates the computations considerably. The region between these two concentric cylinders will be referred to as Region II, the region inside the cylinder $r = r_2$ will be referred to as Region III. At $r = r_1$ and $r = r_2$, continuity conditions apply that yield the boundary conditions needed for the solution of the differential equations to be unique. Unfortunately, the obtained system of differential equations appears to be numerically unstable. In Section 4, we cope with this problem and present a method to trans-

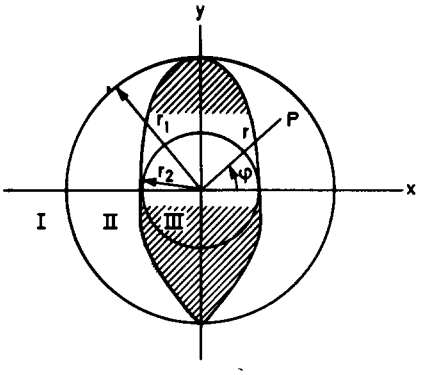

Figure 1. Cross-section of the cylindrical inhomogeneity. The inhomogeneity is enclosed by a cylindrical surface of radius r_1 and the z-axis as axis.

form the system of differential equations into a related one with better stability properties as regards its numerical solution. To illustrate the applicability of the method, the scattering properties of a number of inhomogeneities are computed (Section 6).

The scattering problem under consideration is usually analyzed computationally with the aid of the integral-equation method [1,2,3]. This method, in general, requires a large amount of storage capacity and computation time. An alternative to this is furnished by the unimoment method [4] where, inside a circular cylinder completely surrounding the inhomogeneity the field is computed with the aid of the finite-element method. Outside this cylinder the fields, like in our method, are expanded in terms of the wave functions of the circular cylinder. Although the unimoment method has considerable advantages over the integral-equation method, we believe that, in many cases, our method is still to be preferred because:

(a) The method can be applied with relative ease to a wide range of problems;

(b) Although [4] does not provide computation times for specific problems, we believe that our method, in general, uses a smaller amount of computation time.

Vincent [5] uses a method that is similar to ours in that he, too, combines an expansion of the field, outside a cylinder of radius r_1, in terms of the wave functions of the circular cylinder, with first-order ordinary differential equations inside this cylinder. Our method of arriving at the system of first-order ordinary differential equations appears to be more straightforward, while [5] does not provide a method to cope with the difficulty of numerical instabilities.

2. Description of the configuration

In Section 1 the configuration was divided into three different regions. In Table 1 these regions as well as their permittivities ϵ and permeabilities μ are defined. Relevant wavenumbers are indicated.

We shall consider time-harmonic fields. The complex time factor $\exp(-i\omega t)$, where i is the imaginary unit, ω the angular frequency and t the time, is omitted in the formulas. Since the media in the configuration may be lossy, the constitutive coefficients are, in general, complex with a non-negative imaginary part.

TABLE 1.

Regions in the configuration and their electromagnetic properties

Region	Location $(0 \leqslant \phi < 2\pi, -\infty < z < \infty)$	Permittivity $(\epsilon = \epsilon_0 \epsilon_r)$	Permeability $(\mu = \mu_0 \mu_r)$	Wavenumber $(\mathrm{Re}(k) \geqslant 0)$
Region I	$r_1 < r < \infty$	$\epsilon_0 \epsilon_1$	$\mu_0 \mu_1$	$k_1 = \omega(\epsilon_0 \epsilon_1 \mu_0 \mu_1)^{\frac{1}{2}}$
Region II	$r_2 < r < r_1$	$\epsilon_0 \epsilon_2$	$\mu_0 \mu_2$	$k_2 = \omega(\epsilon_0 \epsilon_2 \mu_0 \mu_2)^{\frac{1}{2}}$
Region III	$0 \leqslant r < r_2$	$\epsilon_0 \epsilon_3$	$\mu_0 \mu_3$	$k_3 = \omega(\epsilon_0 \epsilon_3 \mu_0 \mu_3)^{\frac{1}{2}}$

ϵ_0 and μ_0 denote the permittivity and the permeability, respectively, in vacuo.

3. The electromagnetic-field equations and the related system of differential equations

Outside the region where the sources are located, the electromagnetic fields in the configuration satisfy the source-free electromagnetic-field equations

$$\nabla \times \boldsymbol{H} = -i\omega\epsilon \boldsymbol{E}, \quad \nabla \times \boldsymbol{E} = i\omega\mu \boldsymbol{H}, \tag{1}$$

where $\epsilon = \epsilon(r)$ and $\mu = \mu(r)$ denote the local value of the piecewise continuous permittivity and permeability, respectively. The incident field is assumed to have a z-dependence of the type $\exp(ik_z z)$. Because of the translational invariance of the configuration, all fields in the configuration have this z-dependence in common. In order to obtain, in Region II, a system of first-order ordinary differential equations in the radial variable r, we separate in (1) the radial field components from the field components that are transverse to the radial coordinate and rewrite (1) as

$$\begin{aligned}
\partial_r E_z &= \partial_z E_r - i\omega\mu_0\mu_2 H_\phi, \\
\partial_r H_\phi &= \frac{1}{r}\partial_\phi H_r - i\omega\epsilon_0\epsilon_2 E_z - \frac{1}{r} H_\phi, \\
\partial_r H_z &= \partial_z H_r + i\omega\epsilon_0\epsilon_2 E_\phi, \\
\partial_r E_\phi &= \frac{1}{r}\partial_\phi E_r + i\omega\mu_0\mu_2 H_z - \frac{1}{r} E_\phi, \\
E_r &= (i\omega\epsilon_0\epsilon_2)^{-1}\left(\partial_z H_\phi - \frac{1}{r}\partial_\phi H_z\right), \\
H_r &= (i\omega\mu_0\mu_2)^{-1}\left(\frac{1}{r}\partial_\phi E_z - \partial_z E_\phi\right).
\end{aligned} \tag{2}$$

We note that the field quantities E_z, H_z, H_ϕ and E_ϕ, whose derivatives with respect to r appear in the left-hand side of (2), are piecewise continuous functions of ϕ. These field quantities are expanded in terms of a Fourier series with respect to ϕ. We write

$$
\begin{aligned}
E_z &= \exp(ik_z z) \sum_{m=-\infty}^{\infty} \alpha_m(r) \exp(im\phi), \\
H_\phi &= (k_0/i\omega\mu_0) \exp(ik_z z) \sum_{m=-\infty}^{\infty} \beta_m(r) \exp(im\phi), \\
H_z &= (k_0/i\omega\mu_0) \exp(ik_z z) \sum_{m=-\infty}^{\infty} \gamma_m(r) \exp(im\phi), \\
E_\phi &= \exp(ik_z z) \sum_{m=-\infty}^{\infty} \delta_m(r) \exp(im\phi),
\end{aligned} \tag{3}
$$

with

$$
k_0 = \omega(\epsilon_0\mu_0)^{\frac{1}{2}}, \quad \mathrm{Re}(k_0) \geqslant 0. \tag{4}
$$

Now, substituting (3) in (2), eliminating the field quantities E_r and H_r and using the orthogonality properties of the sequence $\{\exp(im\phi) \mid m = 0, \pm 1, \pm 2, \ldots\}$ over the interval $0 \leqslant \phi < 2\pi$, we obtain a system of differential equations that can be written as

$$
\begin{aligned}
\partial_r \alpha_m(r) &= \Sigma_n V^{(1)}_{m,n}(r)\beta_n(r) + \Sigma_n V^{(2)}_{m,n}(r)\gamma_n(r), \\
\partial_r \beta_m(r) &= \Sigma_n W^{(3)}_{m,n}(r)\alpha_n(r) + \Sigma_n W^{(4)}_{m,n}(r)\delta_n(r) - \frac{1}{r}\beta_m(r), \\
\partial_r \gamma_m(r) &= \Sigma_n W^{(1)}_{m,n}(r)\delta_n(r) + \Sigma_n W^{(2)}_{m,n}(r)\alpha_n(r), \\
\partial_r \delta_m(r) &= \Sigma_n V^{(3)}_{m,n}(r)\gamma_n(r) + \Sigma_n V^{(4)}_{m,n}(r)\beta_n(r) - \frac{1}{r}\delta_m(r),
\end{aligned} \tag{5}
$$

with

$$
\begin{aligned}
V^{(1)}_{m,n}(r) &= \frac{1}{2\pi} \int_0^{2\pi} (k_z^2/k_0\epsilon_2 - k_0\mu_2) \exp(i(n-m)\phi) d\phi, \\
V^{(2)}_{m,n}(r) &= \frac{1}{2\pi} \int_0^{2\pi} (-nk_z/k_0\epsilon_2 r) \exp(i(n-m)\phi) d\phi, \\
V^{(3)}_{m,n}(r) &= \frac{1}{2\pi} \int_0^{2\pi} (k_0\mu_2 - mn/k_0\epsilon_2 r^2) \exp(i(n-m)\phi) d\phi, \\
V^{(4)}_{m,n}(r) &= \frac{1}{2\pi} \int_0^{2\pi} (mk_z/k_0\epsilon_2 r) \exp(i(n-m)\phi) d\phi,
\end{aligned} \tag{6}
$$

and

$$
\begin{aligned}
W^{(1)}_{m,n}(r) &= \frac{1}{2\pi} \int_0^{2\pi} (k_z^2/k_0\mu_2 - k_0\epsilon_2) \exp(i(n-m)\phi) d\phi, \\
W^{(2)}_{m,n}(r) &= \frac{1}{2\pi} \int_0^{2\pi} (-nk_z/k_0\mu_2 r) \exp(i(n-m)\phi) d\phi,
\end{aligned} \tag{7}
$$

$$W^{(3)}_{m,n}(r) = \frac{1}{2\pi}\int_0^{2\pi} (k_0\epsilon_2 - mn/k_0\mu_2 r^2)\exp(i(n-m)\phi)d\phi,$$
$$W^{(4)}_{m,n}(r) = \frac{1}{2\pi}\int_0^{2\pi} (mk_z/k_0\mu_2 r)\exp(i(n-m)\phi)d\phi. \tag{7}$$

Equation (5) constitutes a system of first-order ordinary differential equations. These differential equations are coupled through r-dependent coupling coefficients whose values depend on the type of inhomogeneity in Region II. To construct the values of the field quantities, the differential equations are to be supplemented by a suitable number of boundary conditions. These boundary conditions follow from the continuity of the tangential field components across $r = r_1$ and $r = r_2$. This requires expressions for the field quantities E_z, H_ϕ, H_z and E_ϕ in Regions I and III. In these homogeneous regions the field quantities can be expressed in terms of E_z and H_z. In Region I, E_z and H_z are written as

$$E_z = E_z^i + E_z^s,\ H_z = H_z^i + H_z^s, \tag{8}$$

where E_z^i, H_z^i denote the z-components of the 'incident field', i.e. the field that would exist if no inhomogeneity were present and E_z^s, H_z^s denote the z-components of the 'scattered field', i.e. the field that is due to the presence of the inhomogeneity. Since the incident field is bounded at $r = 0$, it can be expressed in terms of cylindrical wave functions as

$$E_z^i = \exp(ik_z z)\,\Sigma_m A_m^E J_m(\Gamma_1 r)\exp(im\phi),$$
$$H_z^i = (k_0/i\omega\mu_0)\exp(ik_z z)\,\Sigma_m A_m^H J_m(\Gamma_1 r)\exp(im\phi), \tag{9}$$

with

$$\Gamma_1 = (k_1^2 - k_z^2)^{\frac{1}{2}} \text{ with } \mathrm{Re}(\Gamma_1) \geqslant 0 \tag{10}$$

and where $J_{-m}(z) = (-1)^m J_m(z)$. In (9), A_m^E and A_m^H are constants that follow from the prescribed source distribution; they are considered to be known. In the same way the scattered field, outside the cylinder of radius r_1, can be written as

$$E_z^s = \exp(ik_z z)\,\Sigma_m B_m^E H_m^{(1)}(\Gamma_1 r)\exp(im\phi),$$
$$H_z^s = (k_0/i\omega\mu_0)\exp(ik_z z)\,\Sigma_m B_m^H H_m^{(1)}(\Gamma_1 r)\exp(im\phi), \quad \text{in Region I} \tag{11}$$

where $H_{-m}^{(1)}(z) = \exp(im\pi)H_m^{(1)}(z)$ and where B_m^E and B_m^H are as yet unknown constants. Now substituting (9) and (11) in (8), we obtain expressions for E_z and H_z for $r_1 < r < \infty$ in terms of cylindrical wave functions. The corresponding expressions for E_ϕ and H_ϕ are, using (1), obtained as

$$E_\phi = -\exp(ik_z z)\,\Sigma_m \left\{ \frac{mk_z}{\Gamma_1^2 r}\,(A_m^E J_m(\Gamma_1 r) + B_m^E H_m^{(1)}(\Gamma_1 r)) + \frac{k_0\mu_1}{\Gamma_1}(A_m^H J_m'(\Gamma_1 r) + B_m^H H_m^{(1)'}(\Gamma_1 r)) \right\} \exp(im\phi),$$

$$H_\phi = -(k_0/i\omega\mu_0)\exp(ik_z z)\,\Sigma_m \left\{ \frac{k_0\epsilon_1}{\Gamma_1}(A_m^E J_m'(\Gamma_1 r) + B_m^E H_m^{(1)'}(\Gamma_1 r)) + \frac{mk_z}{\Gamma_1^2 r}\,(A_m^H J_m(\Gamma_1 r) + B_m^H H_m^{(1)}(\Gamma_1 r)) \right\} \exp(im\phi), \tag{12}$$

where a dash denotes differentiation with respect to the argument. Using the expressions for E_z and H_z in Region I (eqns. (8), (9) and (11)) and in Region II (eq. (3)), we arrive at expressions for the unknown constants in the expressions (11) for the scattered field by taking the limit $r \downarrow r_1$ in the expressions that hold in Region I and taking the limit $r \uparrow r_1$ in (3) and using the continuity of E_z and H_z at the surface of the cylinder $r = r_1$. In this way we obtain the relations

$$B_m^E = (\alpha_m(r_1) - A_m^E J_m(\Gamma_1 r_1))/H_m^{(1)}(\Gamma_1 r_1),$$
$$B_m^H = (\gamma_m(r_1) - A_m^H J_m(\Gamma_1 r_1))/H_m^{(1)}(\Gamma_1 r_1). \tag{13}$$

Using the continuity of H_ϕ and E_ϕ at $r = r_1$ and eliminating the unknown constants B_m^E and B_m^H from the resulting equations by using (13), we obtain the boundary conditions

$$\frac{2ik_0\epsilon_1}{\pi} A_m^E = k_0\epsilon_1\Gamma_1 r_1 H_m^{(1)'}(\Gamma_1 r_1)\alpha_m(r_1) + \Gamma_1^2 r_1 H_m^{(1)}(\Gamma_1 r_1)\beta_m(r_1) + mk_z H_m^{(1)}(\Gamma_1 r_1)\gamma_m(r_1),$$

$$\frac{2ik_0\mu_1}{\pi} A_m^H = mk_z H_m^{(1)}(\Gamma_1 r_1)\alpha_m(r_1) + k_0\mu_1\Gamma_1 r_1 H_m^{(1)'}(\Gamma_1 r_1)\gamma_m(r_1) + \Gamma_1^2 r_1 H_m^{(1)}(\Gamma_1 r_1)\delta_m(r_1). \tag{14}$$

Having derived the boundary conditions that apply to $r = r_1$ we will now derive the ones that apply to $r = r_2$. Since the fields are bounded at $r = 0$, E_z and H_z can, in Region III, be expressed, in terms of cylindrical wave functions, as

$$E_z = \exp(ik_z z)\,\Sigma_m C_m^E J_m(\Gamma_3 r)\exp(im\phi),$$
$$H_z = (k_0/i\omega\mu_0)\exp(ik_z z)\,\Sigma_m C_m^H J_m(\Gamma_3 r)\exp(im\phi), \quad \text{in Region III} \tag{15}$$

where

$$\Gamma_3 = (k_3^2 - k_z^2)^{\frac{1}{2}} \text{ with } \mathrm{Re}(\Gamma_3) \geqslant 0. \tag{16}$$

In (15), C_m^E and C_m^H are as yet unknown constants. As before, we can express E_ϕ and H_ϕ in terms of E_z and H_z and thus obtain expansions for E_ϕ and H_ϕ in Region III. Using the expressions for E_z and H_z in Region II (eq. (3)) and in Region III (eq. (15)) and using the continuity of E_z and H_z at the surface of the cylinder $r = r_2$, we arrive at expressions for the unknown constants in the expressions (15) for the field in Region III. In this way, we obtain the relations

$$C_m^E = \alpha_m(r_2)/J_m'(\Gamma_3 r_2),\ C_m^H = \gamma_m(r_2)/J_m(\Gamma_3 r_2). \tag{17}$$

Using the continuity of E_ϕ and H_ϕ at $r = r_2$ and eliminating the unknown constants C_m^E and C_m^H from the resulting equations by using (17), we obtain the boundary conditions

$$\begin{aligned} &k_0\epsilon_3\Gamma_3 r_2 J_m(\Gamma_3 r_2)\alpha_m(r_2) + \Gamma_3^2 r_2 J_m(\Gamma_3 r_2)\beta_m(r_2) \\ &\qquad + mk_z J_m(\Gamma_3 r_2)\gamma_m(r_2) = 0, \\ &mk_z J_m(\Gamma_3 r_2)\alpha_m(r_2) \\ &+ k_0\mu_3\Gamma_3 r_2 J_m'(\Gamma_3 r_2)\gamma_m(r_2) + \Gamma_3^2 r_2 J_m(\Gamma_3 r_2)\delta_m(r_2) = 0. \end{aligned} \tag{18}$$

Now the system of differential equations (5), together with the boundary conditions (14) and (18), constitutes a two-point boundary-value problem for the calculation of the field in Region II. Once this problem has been solved, the fields in Regions I and III are computed from (13) and (17). Inspection of the system of differential equations (5), of the coupling coefficients (6) and (7) and of the boundary conditions (14) and (18) reveals that when $k_z = 0$, i.e. when the fields in the configuration are independent of z, the two-point boundary-value problem separates into two, mutually uncoupled, boundary-value problems each containing one half of the number of equations. For the first we have $E_z \neq 0, H_\phi \neq 0, H_z = 0$ and $E_\phi = 0$, generally referred to as the case of E-polarization. For the second we have $E_z = 0, H_\phi = 0, H_z \neq 0$ and $E_\phi = 0$, the case of H-polarization. The governing equations are easily obtained from the equations that have been derived above, by putting $k_z = 0$. In our further analysis we will consider the general case.

The numerical solution of the two-point boundary-value problem can be obtained by using one of the standard techniques, for instance the shooting method, which case the problem is replaced by a related initial-value problem [6,7,8]. However, the relevant initial-value problem turns out to be numerically unstable. Consequently, only inhomogeneities of relatively small dimensions can be dealt with in this way. In Section 4 we shall transform the present two-point boundary-value problem into a different boundary-value problem, the latter having the advantage of leading to an associated initial-value problem that is numerically stable.

4. Transformation of the system of differential equations into one that is stable

In order to cope with the stability problems that are posed by the solution of (5), we introduce new r-dependent functions $e_m^{\pm}(r)$ and $h_m^{\pm}(r)$ that are defined as follows

$$e_m^{\pm}(r) = \alpha_m(r) \pm Z_m \beta_m(r),$$
$$h_m^{\pm}(r) = \gamma_m(r) \pm Z_m \delta_m(r), \tag{19}$$

where

$$Z_m = (r/r_0)\,(m^2 + (r/r_0)^2)^{-\frac{1}{2}}. \tag{20}$$

In (20), r_0 is some positive number that will be chosen later on, such that optimum results are obtained. The differential equations to be satisfied by $e_m^{\pm}(r)$ and $h_m^{\pm}(r)$ are obtained from (5) and (19) as

$$\begin{aligned}
2\partial_r e_m^{\pm} &= \Sigma_n (V_{m,n}^{(1)} Z_n^{-1} \pm (\Lambda_m \delta_{m,n} + Z_m W_{m,n}^{(3)}))e_n^{+} \\
&\quad + \Sigma_n (-V_{m,n}^{(1)} Z_n^{-1} \pm (-\Lambda_m \delta_{m,n} + Z_m W_{m,n}^{(3)}))e_n^{-} \\
&\quad + \Sigma_n (V_{m,n}^{(2)} \pm Z_m W_{m,n}^{(4)} Z_n^{-1})h_n^{+} \\
&\quad + \Sigma_n (V_{m,n}^{(2)} \mp Z_m W_{m,n}^{(4)} Z_n^{-1})h_n^{-}, \\
2\partial_r h_m^{\pm} &= \Sigma_n (W_{m,n}^{(2)} \pm Z_m V_{m,n}^{(4)} Z_n^{-1})e_n^{+} \\
&\quad + \Sigma_n (W_{m,n}^{(2)} \mp Z_m V_{m,n}^{(4)} Z_n^{-1})e_n^{-} \\
&\quad + \Sigma_n (W_{m,n}^{(1)} Z_n^{-1} \pm (\Lambda_m \delta_{m,n} + Z_m V_{m,n}^{(3)}))h_n^{+} \\
&\quad + \Sigma_n (-W_{m,n}^{(1)} Z_n^{-1} \pm (-\Lambda_m \delta_{m,n} + Z_m V_{m,n}^{(3)}))h_n^{-},
\end{aligned} \tag{21}$$

with

$$\Lambda_m(r) = -(r/r_0^2)/(m^2 + (r/r_0)^2); \tag{22}$$

$\delta_{m,n}$ denotes the Kronecker delta. The corresponding transformation of the boundary conditions (14) and (18) leads to

$$\begin{aligned}
\frac{4ik_0\epsilon_1}{\pi} A_m^E &= \Gamma_1 r_1 (k_0 \epsilon_1 H_m^{(1)'}(\Gamma_1 r_1) + \Gamma_1 H_m^{(1)}(\Gamma_1 r_1) Z_m^{-1}(r_1))e_m^{+}(r_1) \\
&\quad + \Gamma_1 r_1 (k_0 \epsilon_1 H_m^{(1)'}(\Gamma_1 r_1) - \Gamma_1 H_m^{(1)}(\Gamma_1 r_1) Z_m^{-1}(r_1))e_m^{-}(r_1) \\
&\quad + m k_z H_m^{(1)}(\Gamma_1 r_1)(h_m^{+}(r_1) + h_m^{-}(r_1)), \\
\frac{4ik_0\mu_1}{\pi} A_m^H &= m k_z H_m^{(1)}(\Gamma_1 r_1)(e_m^{+}(r_1) + e_m^{-}(r_1)) \\
&\quad + \Gamma_1 r_1 (k_0 \mu_1 H_m^{(1)'}(\Gamma_1 r_1) + \Gamma_1 H_m^{(1)}(\Gamma_1 r_1) Z_m^{-1}(r_1))h_m^{+}(r_1) \\
&\quad + \Gamma_1 r_1 (k_0 \mu_1 H_m^{(1)'}(\Gamma_1 r_1) - \Gamma_1 H_m^{(1)}(\Gamma_1 r_1) Z_m^{-1}(r_1))h_m^{-}(r_1),
\end{aligned} \tag{23}$$

$$\begin{aligned}
0 &= \Gamma_3 r_2 (k_0 \epsilon_3 J_m'(\Gamma_3 r_2) + \Gamma_3 J_m(\Gamma_3 r_2) Z_m^{-1}(r_2))e_m^{+}(r_2) \\
&\quad + \Gamma_3 r_2 (k_0 \epsilon_3 J_m'(\Gamma_3 r_2) - \Gamma_3 J_m(\Gamma_3 r_2) Z_m^{-1}(r_2))e_m^{-}(r_2) \\
&\quad + m k_z J_m(\Gamma_3 r_2)(h_m^{+}(r_2) + h_m^{-}(r_2)),
\end{aligned} \tag{24}$$

$$0 = mk_z J_m(\Gamma_3 r_2)(e_m^+(r_2) + e_m^-(r_2)) \tag{24}$$
$$+ \Gamma_3 r_2 (k_0 \mu_3 J_m'(\Gamma_3 r_2) + \Gamma_3 J_m(\Gamma_3 r_2) Z_m^{-1}(r_2)) h_m^+(r_2)$$
$$+ \Gamma_3 r_2 (k_0 \mu_3 J_m'(\Gamma_3 r_2) - \Gamma_3 J_m(\Gamma_3 r_2) Z_m^{-1}(r_2)) h_m^-(r_2).$$

The two-point boundary-value problem defined by the system of differential equations (21) together with the boundary conditions (23) and (24), too, can be solved by using a shooting method [6,7,8]. The initial-value problem obtained in this case, turns out to be numerically stable.

Equation (13) is now replaced by

$$B_m^E = (\tfrac{1}{2}(e_m^+(r_1) + e_m^-(r_1)) - A_m^E J_m(\Gamma_1 r_1))/H_m^{(1)}(\Gamma_1 r_1),$$
$$B_m^H = (\tfrac{1}{2}(h_m^+(r_1) + h_m^-(r_1)) - A_m^H J_m(\Gamma_1 r_1))/H_m^{(1)}(\Gamma_1 r_1), \tag{25}$$

and equation (17) by

$$C_m^E = \tfrac{1}{2}(e_m^+(r_2) + e_m^-(r_2))/J_m(\Gamma_3 r_2),$$
$$C_m^H = \tfrac{1}{2}(h_m^+(r_2) + h_m^-(r_2))/J_m(\Gamma_3 r_2). \tag{26}$$

As to the transformation (19) we note that it was ultimately chosen such that it serves a twofold goal.

Primarily the transformation was designed to overcome the stability difficulties posed by the solution of (5). The fact that the system of differential equations (5) turns out to be numerically unstable, can be explained by investigating the value of the elements of the coefficient matrices in the differential equations as well as the convergence properties of the expansions in (3). It can be observed from (6) and (7) that the diagonal elements of $(V_{m,n}^{(3)})$ and $(W_{m,n}^{(3)})$ are approximately proportional to m^2, whereas those of $(V_{m,n}^{(1)})$ and $(W_{m,n}^{(1)})$ do not depend on m. The behavior of the elements of the other matrices is such that they do not contribute to the instable behavior of (5). The properties of the matrices $(V_{m,n}^{(3)})$ and $(W_{m,n}^{(3)})$ cause the convergence of the expansions of E_z in terms of α_m and H_z in terms of γ_m to be much better than the convergence of the expansions of E_ϕ in terms of δ_m and H_ϕ in terms of β_m. As a consequence of the relatively slow convergence of the β_m and δ_m series, combined with the properties of the matrices $(V_{m,n}^{(3)})$ and $(W_{m,n}^{(3)})$, an appreciable loss of accuracy will occur when carrying out those summations in (5) that have to do with the elements of the matrices $(V_{m,n}^{(3)})$ and $(W_{m,n}^{(3)})$, in particular for large values of $|m|$. The fact that this first goal is attained by using the transformation (19) can be explained by studying the resulting system of differential equations (21). In (21), the diagonal elements of all coefficient matrices were approximately proportional to m, whereas the convergence properties of $e_m^\pm$ and $h_m^\pm$ are identical. Because of this, the summations in (21) do not suffer from an appreciable loss of accuracy and consequently the initial-value problem related to (21) behaves numerically in a stable manner.

A second consideration concerning the transformation, is related to the r-dependence of the coefficient matrices in (5) and (21). The transformation was chosen such that the elements of the matrices in (21) show a dependence on r of the order $1/r$ at small values of r, whereas the

elements of the matrices $(V^{(3)}_{m,n})$ and $(W^{(3)}_{m,n})$ show a dependence on r of the order $1/r^2$ as $r \to 0$. The latter fact may cause additional numerical difficulties, in particular for small values of r. For larger values of r, the transformation does not substantially influence the behavior of the elements of the coefficient matrices.

As to the choice of r_0 in (20) and (22) we mention that numerical experiments indicate that it should be chosen as $r_0 = 1/k_0$. This choice, however, turns out to be a not very critical one.

5. Discussion of the numerical techniques

In solving the scattering problem under consideration, numerical problems of two different kinds are encountered and need some discussion. The first one is posed by the evaluation of the integrals in (6) and (7). When the inhomogeneity consists of a piecewise homogeneous medium, ϵ_2 and μ_2 will have a piecewise constant value over the interval of integration and consequently the integration can be carried out analytically. When the inhomogeneity consists of an inhomogeneous medium of such a kind that the integration cannot be carried out analytically, the interval of integration is divided into a number of segments that are chosen so small that, in each segment, ϵ_2 and μ_2 can be approximated with sufficient accuracy by either a constant or a function that varies linearly with ϕ. Over each segment, the integrations can then be carried out analytically and the integrals over $0 \leqslant \phi < 2\pi$ follow as the sum of the integrals over the various segments. The second numerical problem lies in the numerical solution of the two-point boundary-value problem defined by (21), (23) and (24). This boundary-value problem is solved using a shooting method [8] that replaces the problem by an initial-value problem. The initial-value problem is solved in the direction of increasing r starting from $r = r_2$. For this, we have used the classical fourth-order Runge-Kutta formula [9]. The stepsize in the numerical integrations and the number of terms taken into account in the Fourier series [e.g. in (3)] have been chosen such that our final accuracy proved to be within a few percent. All computations have been carried out in single-precision arithmetic on the IBM-370/158 computer of the Computing Center of the Delft University of Technology.

Several checks on the computer program and on the computational results have been carried out in order to eliminate possible errors. We mention some of them.

(1) *Reciprocity.* In reciprocal configurations (to which class our inhomogeneities belong), scattered fields that pertain to two different incident fields should satisfy certain reciprocity relations. These relations were satisfied to within about five significant figures.

(2) *Geometrical symmetry.* In many cases, the inhomogeneity shows a number of geometrical symmetry properties. Scattered fields that are associated with incident fields that comply with the geometrical symmetry, should reflect this symmetry. This condition, too, was satisfied.

(3) *Convergence of numerical procedures.* The accuracy of a numerical integration depends on the number of segments (in (6) and (7)) or on the stepsize (in (21)) that is chosen. The relation, which is known from numerical analysis, between the number of segments and the stepsize on the one hand and the accuracy of the result on the other, proved to be consistent with the one obtained from the actual numerical results.

(4) *Solving the scattering problem in different ways, using our method.* By choosing the origin of the coordinate system at two or more different locations in the cross-section of the in-

geneity, we obtain numerically independent scattering problems that should, after performing appropriate transformations, have the same solution. This condition was satisfied within the accuracy of the solution of the scattering problem. (This accuracy can, of course, be improved at the cost of extra computation time and storage requirements.)

(5) *Comparison of our results with those that have been obtained by using other methods.* Results that have been obtained by using our method of solution are compared with those that have been reported in papers that deal with other numerical techniques [1,2,3,4]. Our results are found to be in accordance with computational results presented in [1], [2] and [3]. Discrepancies have been found between our results and some of the results presented in [4]. More detailed comments on this are give in Section 6.

Finally we should consider the number of terms $2M + 1$ (i.e., $m = 0, \pm 1, ..., \pm M$) that are taken into account in the Fourier series in (3), (9), and other equations. Firstly, from the properties of the Hankel functions (see eq. (11)) it follows [10] that M should be chosen slightly larger than $\Gamma_1 r_1$ for optimum results. A second factor that determines the choice of M follows from the analysis of the numerical values of the coefficients in the Fourier series in (3). This analysis leads in many cases to approximately the same value of M. However, in configurations where the inhomogeneity shows strong local variations in the permittivity and/or permeability, the series in (3) converge relatively slowly and a larger number of terms has to be taken into account in order to arrive at the desired accuracy.

6. Numerical results

In this section, numerical results pertaining to a number of different cylindrical inhomogeneities are presented. The scattering properties of the inhomogeneities will characterized by the far-field radiation pattern of the scattered fields. At large distances from the cylindrical inhomogeneity ($\Gamma_1 r \gg 1, r \gg r_1$), the scattered fields can be written as

$$\begin{aligned} E_z^s &= (2/\pi\Gamma_1 r)^{\frac{1}{2}} \exp(i(\Gamma_1 r - \pi/4)) \exp(ik_z z) g^E(\phi), \\ H_z^s &= (2/\pi\Gamma_1 r)^{\frac{1}{2}} \exp(i(\Gamma_1 r - \pi/4)) \exp(ik_z z) g^H(\phi), \end{aligned} \tag{27}$$

where the far-field scattering patterns $g^E(\phi)$ and $g^H(\phi)$ are given by

$$\begin{aligned} g^E(\phi) &= \Sigma_m B^E \exp(im(\phi - \pi/2)), \\ g^H(\phi) &= (k_0/i\omega\mu_0) \Sigma_m B_m^H \exp(im(\phi - \pi/2)). \end{aligned} \tag{28}$$

These definitions have been chosen in accordance with the definition of the far-field scattering pattern in [4] in order to facilitate a comparison between our results and the ones presented in [4].

In each of the problems to be solved, the incident field is chosen to a be uniform plane wave. In the cases of E- and H-polarization the incident fields have been chosen such that either $E_z^i = 1$ or $H_z^i = 1$ at the origin of the coordinate system. We have investigated the following configurations.

(1) *A circular cylinder with its center offset from the origin.* Exact solutions for this configuration can be obtained using the method of separation of variables [11]. An excellent agreement with these solutions was obtained for the general case ($k_z \neq 0$) as well as for the cases of E- and H-polarization.

(2) *An inhomogeneous dielectric cylinder.* The second configuration we have investigated, is an inhomogeneous dielectric cylinder in free space [4] having a relative permittivity (see Table 1) $\epsilon_r = (5 - 4(x/a)^2)/(1 + 4(y/a)^2)$, (see Fig. 2). Results for this configuration have been obtained for E- and for H-polarization. We have chosen the free-space wavelength of the incident field such that $a = 0.229\lambda$ where a denotes the radius of the inhomogeneous cylinder. By comparing our results, for the case of E-polarization, with those of [4], this wavelength has been chosen such that it is expected to be approximately equal to the wavelength of the incident field in [4]. However, although some agreement between our results and those in [4] is observed in the case of E-polarization, our results for the case of H-polarization differ considerably from the ones presented in [4]. As to Region III, we mention that we have chosen $r_2 = 0.1\, r_1 = 0.1a$. Inside this region, we have approximated the permittivity ϵ_r by its value at the axis. The error resulting from this approximation is negligible. The computation time for each problem amounts to about three seconds.

(3) *Homogeneous dielectric cylinders of rectangular or elliptic cross-section.* In Figs. 3, 4, 5 and 6 we present the scattering properties of dielectric cylinders of either rectangular or elliptical cross-section. For reasons of comparison, the dimensions of the inhomogeneities, the material properties and the wavelength of the incident fields have been taken from [4]. Discrepancies exist between our results and those presented in [4]. The computation time amounts to about five seconds for the rectangular cylinder and to about forty seconds for the elliptic cylinder.

(4) *A cylindrical vacuum inclusion of elliptic cross-section in a homogeneous medium.* The last configuration to be investigated is a cylindrical vacuum inclusion of elliptic cross-section in a homogeneous medium having a permittivity $\epsilon_r = 2.25$.

In Figs. 7 and 8 we present the results for E- and H-polarization, respectively. In these figures λ denotes the wavelength of the incident wave in the medium that surrounds the vacuum inclusion. The computation time amounts to about ten seconds for the case $a = 0.5\lambda$ (see Figs. 7 and 8) and forty-five seconds for the case $a = \lambda$. Finally, we compute the field scattered by a vacuum inclusion if the incident uniform plane wave has a z-dependence of the form $\exp(ik_z z)$, $k_z \neq 0$. The electric field vector E^i and the wave vector of the incident field lie in in a plane through the z-axis. Consequently, the magnetic field vector H^i is normal to this plane. The between the electric field vector and the positive z-direction is 24.6 degree. Again, ϕ denotes the angle between the plane through the z-axis mentioned above and the plane $y = 0$. In Figs. 9 and 10 we present the far-field scattering patterns of the electric and magnetic fields respectively. These patterns have been normalized with respect to the amplitude of the incident electric and magnetic field respectively. The computation time for this problem amounts to about two hundred seconds.

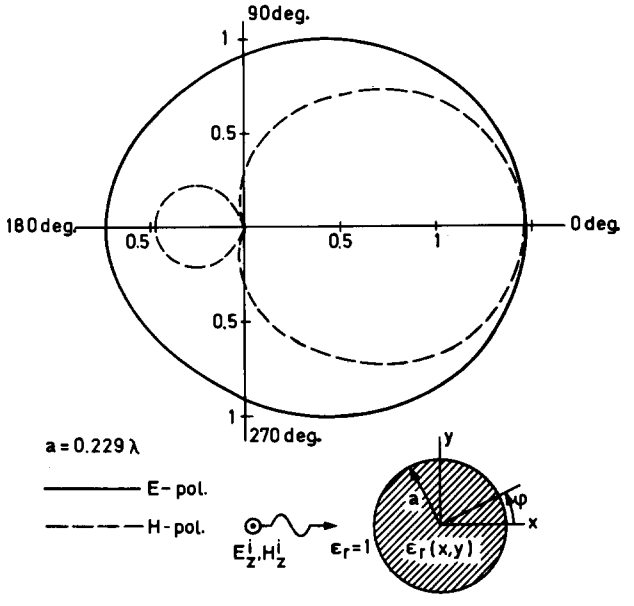

Figure 2. Far-field scattering pattern $|g^E(\phi)|$ and $|g^H(\phi)|$ of an inhomogeneous cylinder with $\epsilon_r = (5 - 4(x/a)^2)/(1 + 4(y/a)^2)$.

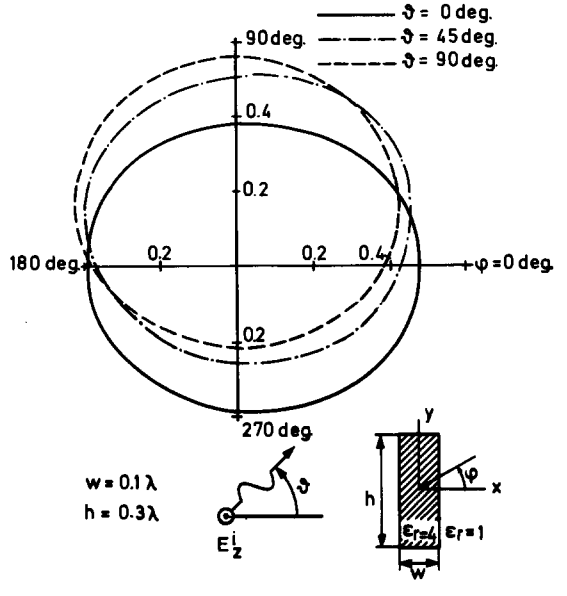

Figure 3. Far-field scattering pattern $|g^E(\phi)|$ of a homogeneous dielectric cylinder with rectangular cross-section, E-polarization.

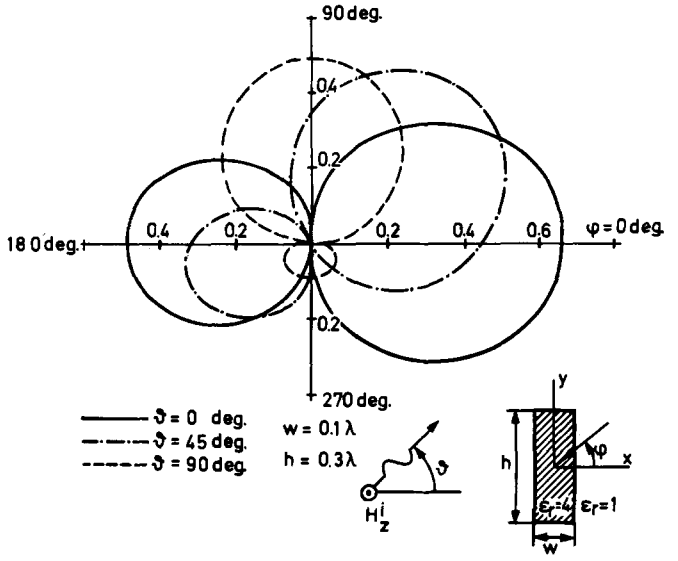

Figure 4. Far-field scattering pattern $|g^H(\phi)|$ of a homogeneous dielectric cylinder with rectangular cross-section, H-polarization.

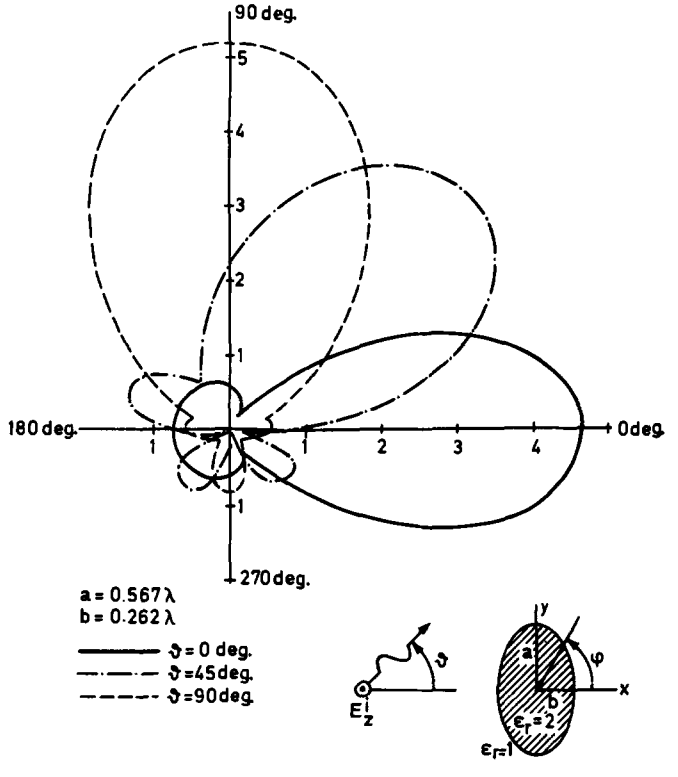

Figure 5. Far-field scattering pattern $|g^E(\phi)|$ of a homogeneous dielectric cylinder with elliptic cross-section, E-polarization.

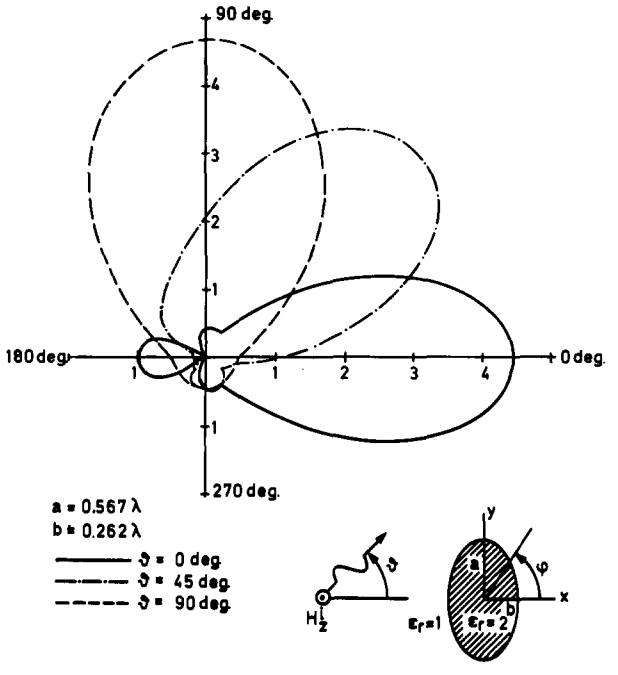

Figure 6. Far-field scattering pattern $|g^H(\phi)|$ of a homogeneous dielectric cylinder with elliptic cross-section, H-polarization.

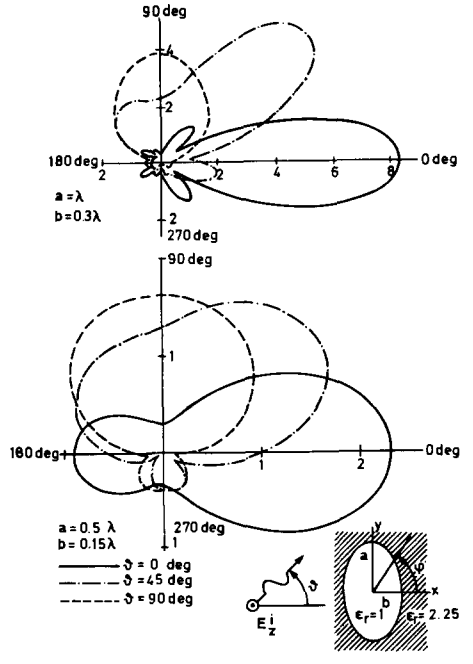

Figure 7. Far-field scattering pattern $|g^E(\phi)|$ of a cylindrical vacuum inclusion of elliptic cross-section in a homogeneous medium, E-polarization.

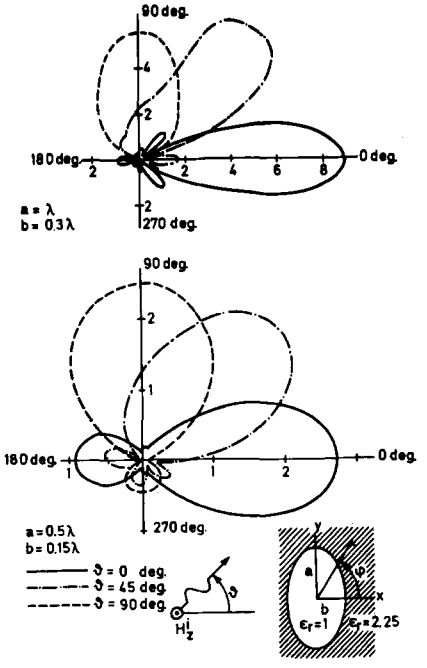

Figure 8. Far-field scattering pattern $|g^H(\phi)|$ of a cylindrical vacuum inclusion of elliptic cross-section in a homogeneous medium, H-polarization.

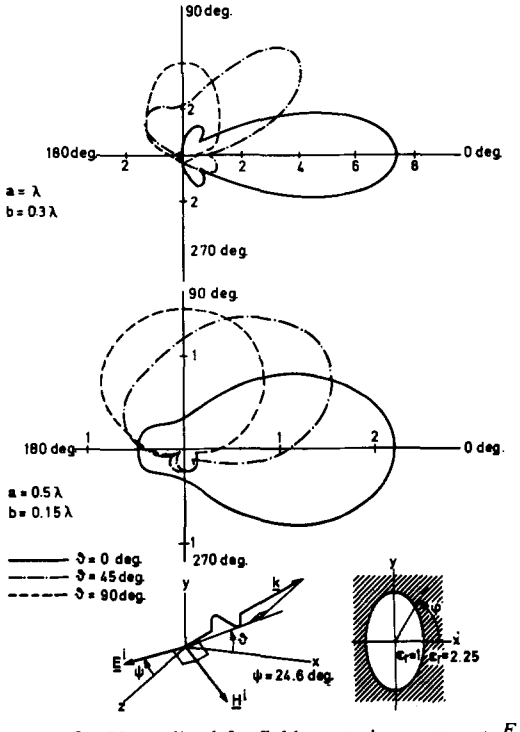

Figure 9. Normalized far-field scattering pattern $|g^E(\phi)|/|E^i|$ of a cylindrical vacuum inclusion of elliptic cross-section in a homogeneous medium with an obliquely incident plane wave.

7. Conclusions

In this paper a method is presented for computing numerically the time-harmonic fields in the presence of a cylindrical transparent inhomogeneity in an otherwise homogeneous medium of infinite extent. The method presented requires, in general, a relatively small amount of computation time and storage capacity. As to the computation times mentioned in Section 6, we note that they can be reduced substantially by taking into account geometrical symmetry, if present, of the scattering inhomogeneities. Another advantage of the method is its flexibility. For a specific problem only a subroutine, which is generally very simple, need be written for the computation of the integrals in (6) and (7), the major part of the main problem therefore remains unchanged. For obstacles that show strong local variations in their permittivity and/or their permeability, a large number of terms in the Fourier expansions has to be taken into

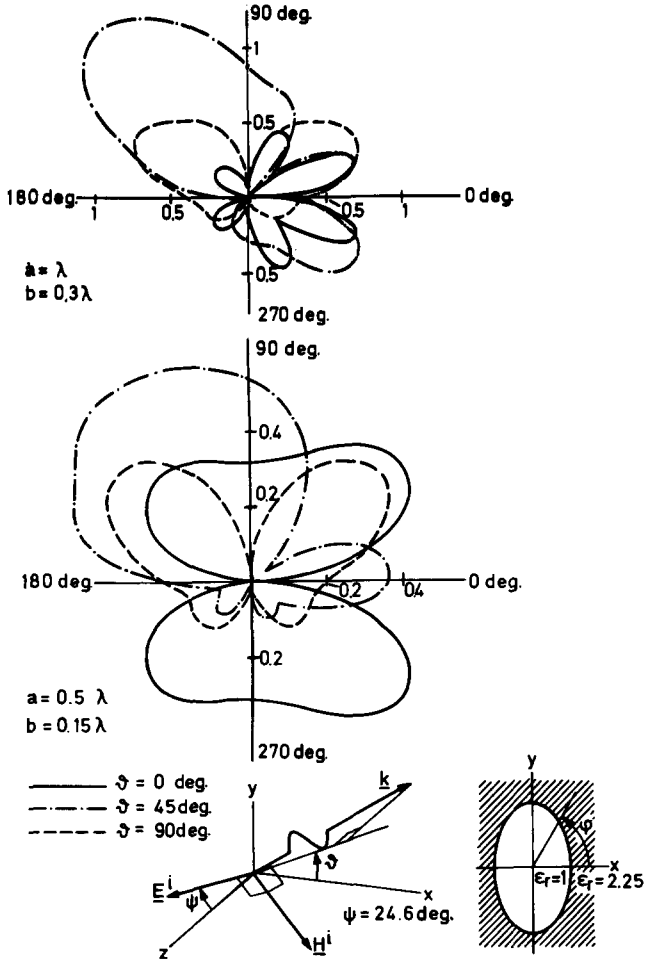

Figure 10. Normalized far-field scattering pattern $|g^H(\phi)|/|H^i|$ of a cylindrical vacuum inclusion of elliptic cross-section in a homogeneous medium with an obliquely incident plane wave.

account in order to arrive at the desired accuracy and this, even with our method, leads to considerable computation times. But then, in the general case $k_z \neq 0$, no attractive alternative is available either. Another limitation seems to be that the method cannot be generalized to problems involving perfectly conducting obstacles. For the latter type of obstacle and in the general case $k_z \neq 0$, the integral-equation method still seems to be the only method of a general nature. However, when the inhomogeneity has a perfectly conducting part with a circular cross-section, the location of the origin of the coordinate system and the radius r_2 can be chosen such that Region III coincides with the conducting cylinder. Now this scattering problem can be solved replacing the boundary conditions (24) by

$$e_m^+(r_2) + e_m^-(r_2) = 0, \quad h_m^+(r_2) - h_m^-(r_2) = 0. \tag{29}$$

For some configurations numerical inaccuracies are observed when solving the two-point boundary-value problem with a shooting method. As an example, we mention the plane dielectric slab as considered in [1] and [12]. For this configuration we were able, with a limited accuracy, to reproduce Richmond's results for the case of E-polarization [1]. For the case of H-polarization [12], however, we did not succeed in reproducing Richmond's results owing to numerical inaccuracies. The latter are due to the fact the system of algebraic equations that has to be solved when applying a shooting method, is ill-conditioned. This problem can be coped with by using, at certain instances during the solution of the system of differential equations, a reorthonormalization of the initial-value problems by the Gram-Schmidt process [13].

Finally, we note that on a previous occasion, essentially the same method was succesfully applied to a number of three-dimensional waveguide discontinuity problems [14].

Acknowledgement

The author whishes to thank Professor A. T. de Hoop for stimulating discussions and suggestions concerning the research presented in this paper.

REFERENCES

[1] J. H. Richmond, Scattering by a dielectric cylinder of arbitrary cross-section shape, *IEEE Trans. Antennas Propagat.* AP-13 (1965) 334-341.
[2] N. K. Uzunoglu, and A. R. Holt, The scattering of electromagnetic radiation from dielectric scatterers, *J. Phys. A.* 10 (1977) 413-424.
[3] W. Tabbara, Light scattering by a single cylindrical lens: numerical results from a rigorous theory, *J. Opt. Soc. Am.* 63 (1975) 17-24.
[4] Shu-Kong Chang and K. K. Mei, Application of the unimoment method to electromagnetic scattering of dielectric cylinders, *IEEE Trans. Antennas Propagat.* AP-24 (1976) 35-42.
[5] P. Vincent, Singularity expansions for cylinders of finite conductivity. To appear in *Applied Physics.*
[6] S. M. Roberts, and J. S. Shipman, *Two-point boundary-value problems: shooting methods,* New York, American Elsevier, 1972, p. 6, Chapter 2.
[7] H. B. Keller, *Numerical methods for two-point boundary-value problems,* Waltham, Blaisdell Publishing Company, 1968, p. 38, Chapter 2.
[8] G. Hall and J. M. Watt, *Modern numerical methods for ordinary differential equations,* Oxford, Clarendon Press, 1976, p. 216, Chapter 16.

[9] G. Hall and J. M. Watt, *Modern numerical methods for ordinary differential equations*, Oxford, Clarendon Press, 1976, p. 4, Chapter 1.

[10] D. R. Wilton and R. Mittra, A new numerical approach to the calculation of electromagnetic scattering properties of two-dimensional bodies of arbitrary cross-section, *IEEE Trans. Antennas Propagat.*, AP-20 (1972) 310-317.

[11] A. C. Lind and J. M. Greenberg, Electromagnetic scattering by obliquely oriented cylinders, *J. Appl. Phys.* 37 (1966) 3195-3203.

[12] J. H. Richmond, TE-wave scattering by a dielectric cylinder of arbitrary cross-section shape, *IEEE Trans. Antennas Propagat.* AP-14 (1966) 460-464.

[13] S. M. Roberts and J. S. Shipman, *Two-point boundary-value problems: shooting methods*, New York, American Elsevier, 1972, p. 71, Chapter 4.

[14] G. Mur, A differential-equation method for the computation of the electromagnetic scattering by an inhomogeneity in a cylindrical waveguide, *Journal of Engineering Math.* 12 (1978) 157-175.